Environ. Sci. Technol. **2006**, *40,* 837−843

Gross Photoreduction Kinetics of Mercury in Temperate Freshwater Lakes and Rivers: Application to a General Model of DGM Dynamics

N. J. O'DRISCOLL,*,† S. D. SICILIANO,‡ D. R. S. LEAN,§ AND M. AMYOT†

Département des sciences biologiques, Université de Montréal, 90 Vincent d'Indy, Montréal, QC, Canada, H2V 2S9, Department of Soil Science, University of Saskatchewan, 51 Campus Drive, Saskatoon, SK, Canada, S7N 5A8, and Biology Department, Faculty of Science, University of Ottawa, P.O. Box 450, Stn. A., Ottawa, ON, Canada, K1N 6N5

Previous published measurements of mercury photoreduction are for net-photoreduction, since photooxidation processes occur simultaneously. In this research we combine continuous dissolved-gaseous mercury (DGM) analysis with a photoreactor and a quartz sparger in order to derive mercury gross photoreduction rate constants for UVB and UVA irradiations. The DGM concentration in each filter-sterilized freshwater was measured at 5 min intervals over a period of 23 h. Photoreduction proceeded for the initial 200 min, after which, reducible mercury was depleted in the sample. Substantial losses in DOC fluorescence were observed during the incubations for UVA radiation but not for UVB; therefore, UVB photoreduction dynamics are not linked to a loss in DOC fluorescence. Pseudo first-order reaction kinetics fit the data well ($r^2 > 0.87$). The rate constants appear divided between lakes and rivers with the mean lake UVB rate constant ($k_{UVB} = 8.91 \times 10^{-5}$ s^{-1}), significantly less than the mean rate constant ($k_{UVB} = 1.81 \times 10^{-4}$ s^{-1}) for the river samples. However, while there were differences for the UVB rates between lakes and rivers, the mean and median rate constants for UVA in lakes ($k_{UVA} = 7.76 \times 10^{-5}$ s^{-1}) did not differ significantly from the mean rate constant for the river sites ($k_{UVA} = 1.78 \times 10^{-4}$ s^{-1}). Here, we propose a model for mercury photoredox dynamics for both temperate lake and river systems. The lake model was validated using principal axis analysis to compare observed and predicted DGM data ($n = 279$) from a variety of lake sites in Nova Scotia and Central Quebec. Principal axis analysis found a linear fit (correlation = 0.81; slope = 2.13) between predicted and observed environmental DGM values when log-normalized. The constant bias on the predicted values was attributed to estimates of available reducible mercury and the effect of DGM volatilization on observed data.

Introduction

Mercury is a ubiquitous environmental contaminant, and it exists in several different forms in the environment. The three major forms of mercury are elemental mercury (Hg^0), inorganic mercury (Hg^{2+}), and methyl mercury (CH_3Hg^+). Elemental mercury is volatile and it is the main form of mercury found in the atmosphere, while inorganic mercury is the predominant form found in water, bound to various organic and inorganic ligands (*1*). Volatilization of dissolved elemental mercury (DGM, dissolved-gaseous mercury) from water is a significant process in the global distribution of mercury. Mason et al. (*2*) has demonstrated the importance of mercury volatilization from the ocean surface and, more recently, has measured the re-deposition of reactive mercury species, which may balance this process (*2*, *3*). O'Driscoll et al., (*4*) demonstrated that current predictive models of mercury volatilization from water are largely driven by the wind speed and the amount of DGM present in the water system. DGM photoproduction begins early in the day and the rate of net DGM production slowly levels to a plateau by sunset (*5*). This plateau is largely assumed to be the result of a balance between photoreduction and photooxidation reactions driven by both abiotic and biotic mechanisms (*6*−*12*). To date, no research has decoupled these two competing processes in order to produce a predictive model for DGM formation based on fundamental rate constants for gross photoreduction and gross photooxidation.

Most methods of discrete (*6*, *13*) and continuous DGM analysis (*4*, *14*−*16*) involve the removal of previously formed DGM in the sample. The DGM concentration measured in these samples is the net result of photoreduction and photooxidation reactions. Therefore, the kinetic analysis of such data represents only rates of net-photoreduction. Researchers have measured net photoreduction of mercury in saltwater (*17*−*20*) and freshwater (*6*, *7*, *11*), in temperate lakes and rivers (*6*, *7*, *21*, *22*), in arctic lakes (*23*), and in southern wetlands (*13*), yet the mechanisms by which it occurs are not well understood.

One approach to decoupling these reactions is to remove the Hg(0) from the reaction vessel as it is forming, thereby depriving the photooxidation reaction of its substrate. Allard and Arsenie (*24*) as well as Vette (*25*) were able to produce continuous reduction using this technique. Rolfhus (*26*) and Xiao et al. (*27*) also used continuous bubbling methodology for DGM analyses, however, there are no published studies of mercury gross photoreduction rates and their application to predictive modeling. Alternatively, there is also promise in the use of stable isotopes for separating competing processes for mercury speciation. For example, Hintelmann and Evans (*28*) demonstrated how stable mercury isotopes might be used to measure specific competing speciation processes such as methylation and demethylation. However, it is not clear how to obtain a stable isotopic standard for dissolved elemental mercury and ensure no photooxidation of the solution.

Many current predictive models for mercury flux are inaccurate when compared with measured data (*4*). In addition, many of the current regional and global mercury fate models lack the fundamental gross photoreduction reaction rates. Yet, the evasion of DGM from waters is typically modeled based on DGM levels in water. To model DGM formation and rates of mercury volatilization from ecosystems, reliable measurements of mercury photoreduction and photooxidation rates are required. Our objective here was to develop a nonchemical method for the de-coupling of

* Corresponding Author current address: Environment Canada, Existing Substances Branch, 20th Floor Place Vincent Massey, 351 St. Joseph Boulevard, Gatineau, Quebec, K1A OH3; phone: (819) 934-6908; fax: (819) 953-4963; e-mail: Nelsoon.ODriscoll@ec.gc.ca.
† Université de Montréal.
‡ University of Saskatchewan.
§ University of Ottawa.

10.1021/es051062y CCC: $33.50
Published on Web 12/22/2005

mercury photoreduction and photooxidation dynamics so that gross photoreduction rates could be obtained using controlled constant radiation sources. We hypothesized that this technique would allow us to determine gross photoreduction rates for UVB and UVA irradiation at a variety of freshwater sites, and thereby develop a predictive DGM model.

Experimental Section

Water Sampling. Water (25 L) was collected from each freshwater site using high-density polyethylene containers that were pre-cleaned with double-deionized (d.i.) water. This has been shown to be an effective way to minimize mercury contamination from containers (*29*) while minimizing the introduction of chemicals that may alter mercury reduction reactions. These sites provide a wide range of dissolved organic carbon concentrations and conductivity measurements (Table SI-1), which have been shown to be important to DGM formation (*5*). In addition literature values for DGM formation are available for several of these sites (*10*, *22*, *29*). Water samples were stored in a dark cold room at 4 °C. When possible, all samples and sample replicates were analyzed within 1 week of collection of the bulk water sample. The analysis of DGM production with UVB irradiation was performed for each sample site followed by a separate analysis for UVA. The longer storage times for samples prior to the UVA irradiation experiments resulted in some losses of total mercury in the bulk water sample prior to analysis (as seen in Table SI-2). This was attributed to microbial reduction and volatilization of elemental mercury.

All sampled water was sterilized immediately prior to analysis using a PE Lab tangential flow system (Pall Corporation), which is constructed with ultra-high molecular weight polyethylene. All tubing was polytetrafluoroethylene (PTFE) , with the exception of a 20 cm piece of polypropylene used for the peristaltic pump. Omega polyethersulfone cassette filters were used to remove all particles greater than 0.2 μm. The 0.2 μm filter was used with an inlet pressure of 8 PSI and no backpressure. This has been shown to be an effective technique to produce water that contains insignificant microbial activity for up to 8 h (*30*).

Photo-Reactor Design and Analysis Methods. A continuous dissolved gaseous mercury analysis system, previously detailed by O'Driscoll et al. (*16*), was modified with a quartz sparger. The sparger consists of a quartz glass cylinder (10.3 cm in height, 8 cm outer diameter, and 2 mm thick) with a polycarbonate flat bottom and a platinum cured silicone stopper in the top (517 cm^3 total volume) (Figure SI-1). The inlet 1/4 inch PTFE tubing was connected to a coarse glass air diffuser and the outlet connects directly to the 1/4 inch PTFE tubing. This quartz sparger was placed in a temperature controlled photochemical irradiation chamber (LuzChem ICH-2 photo reactor) with internal UV meter (Ideal-Sperry 61-680), and temperature was maintained at 25 °C (±1 °C) throughout all analysis incubations using an internal exhaust fan. The photoincubation unit was equipped with a maximum of 8 UVB or UVA bulbs (4 on each side of the quartz sparger, see Figure SI-1). In this way, samples could be analyzed for DGM as it is produced by photoreduction reactions. A typical analysis would consist of blanking the system, analysis of the initial DGM in the sample in the dark, then irradiation of the sample for 24 h and measurement of DGM produced during each 5 minute interval. In this way, a high level of detail was available (n = 288 DGM readings) were available for each sample analysis. Each sterilized sample was analyzed for 24 h in the photoreactor for either UVA or UVB radiation. Ottawa River samples were analyzed in triplicate for each UVA and UVB incubation in order to assess the typical amount of analytical error involved with each incubation.

Blanking of System and Mercury Mass Balance. All PTFE tubing and the quartz sparger were initially acid washed twice in 10% trace HCl for 24 h prior to analysis and then washed with copious amounts of d.i. water. Zero-Hg air blanks analyzed with the sparger exposed to UVB light indicated that mercury was being released even after stringent cleaning procedures. The system was initially run with mercury-free air and UV radiation until mercury readings were undetectable (<0.01 ng m^{-3}). This extra cleaning procedure took 440 min of irradiation with a zero-Hg air flow of 1 L min^{-1} through the sparger. During that time 334 pg of elemental mercury was released from the 10 in. of exposed PTFE tubing and quartz sparger (53% released in the first 120 min). In subsequent analysis, irradiating the empty sparger released no additional mercury.

The glass sparger was also acid rinsed with 10% HCl between sample analyses to determine if substantial mercury was irreversibly bound to the sparger walls. Mercury-free air was then passed through the sparger while irradiating with UVB and UVA radiation and analyzed for mercury. This technique was employed after each sample analysis, and mercury levels were monitored until undetectable.

Analysis Theory. As described by O'Driscoll et al. (*5*) net DGM production in natural waters can be described in the following equation:

$$Hg_{reducible} + \text{photo-reductants} \leftrightarrow DGM + \text{photo-oxidants} \quad (1)$$

In most of the published DGM literature, the analysis is performed after incubation in solar radiation or artificial radiation. Photoreduction and photooxidation are simultaneous competing processes; therefore, these previous measurements are of net DGM produced. In this technique, we are continuously removing DGM as it is formed in solution, thereby pushing eq 1 primarily toward reduction. If we assume that the photoreductants are in excess, then eq 1 can be written as eq 2 (no longer an equilibrium equation). We

$$Hg_{reducible} \rightarrow DGM \quad (2)$$

hypothesized that cumulative DGM would increase in the samples until either photoreductants or available mercury was exhausted and a level plateau was reached. Since we are using a constant irradiation source the gross photoreduction rate constant could be derived from this curve.

Calculation of Irradiance. Scans of spectral irradiance (using an Optikon OL 754 spectra radiometer) and calibration details for the UVB and UVA sources are provided in Figure SI-2. In addition, absorbance scans (280−800 nm at 2 nm intervals) measured for the quartz sparger found no significant (<0.1%) loss of radiation at any wavelength. The radiant flux received by the quartz sparger was calculated using the following equation:

$$\text{radiant energy received (J)} = n\,\text{AET} \quad (3)$$

Where, n is the number of lamps used for irradiation, A is the cross sectional area of the quartz sparger (84.2 cm^2), E is the radiant energy flux from one lamp for the respective wavelength range measured (W cm^{-2}), and T is the interval for DGM analysis (300 s).

The radiation energy in our photoincubator configurations was compared to the radiation received during a typical sunny day in mid summer at our latitude (unpublished data from O'Driscoll et al., ref *5*). Three UVB lamps produced a constant radiant UVB (280−320 nm) output to the sparger of 3.4 J per 5 minute interval, or 90% of average daily full sun exposure. Eight UVA lamps produced a total constant radiant UVA (320−400 nm) output of 54.4 J per 5 minute sample, or 79% of average daily full sun exposure.

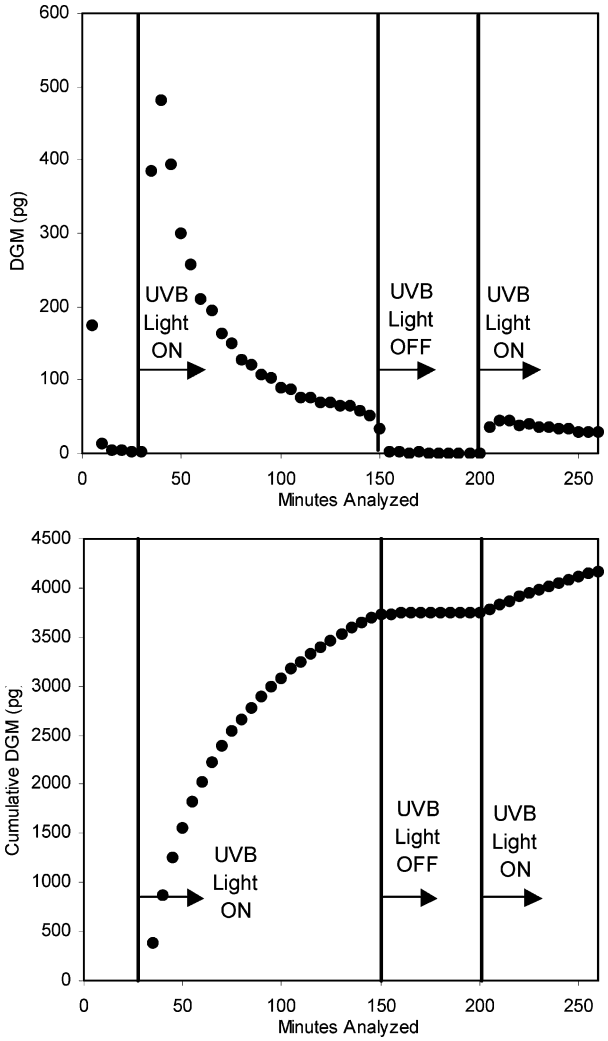

FIGURE 1. Cumulative DGM production and the effects of short interruptions in UVB irradiation. Sample consisted of 300 mL Ottawa River water spiked with 10 000 pg of Hg(II) and 1.2 mg of humic acid.

Effects of Irradiation Intensity and Breaks in Irradiation. To examine the effects of a break in irradiation on DGM production, 100 μL of a 100 μg L^{-1} Hg(II) solution in dilute HNO_3 was spiked into a 300 mL sample of 0.2 μm filtered Ottawa River water. Therefore a minimum of 10 000 pg of Hg(II) was available for photoreduction. Since dissolved organic matter (DOM) is commonly implicated as a mediator of photoreactions we increased the DOM concentration by adding 1.2 mg of humic acid sodium salt (Alfa Aesar) to ensure that this was not a limiting factor. The samples were exposed to high UVB radiation (583% average full sun) with a 60 minute interruption in irradiation (Figure 1) and normal UVB radiation (90% average full sun) with a 24 hour break in irradiation.

To determine if radiation intensity would affect the reactions kinetics, Ottawa River samples were analyzed at three different intensities of UVB radiation (61, 90, and 137% average full sun) and the rate constants were calculated.

Analysis of Total Mercury, DOC Concentration, and DOC Fluorescence (DOCF). Samples before and after each irradiation were collected in 50 mL polypropylene centrifuge tubes and analyzed for DOC, DOCF, and total mercury. Total mercury samples were preserved with 0.5% BrCl (*31*) and analyzed using a Tekran 2600 (cold vapor atomic fluorescence) analyzer. DOC samples were kept cold until analysis by 100 °C persulfate wet oxidation and CO_2 detection by infrared spectroscopy (OI Corporation Model 1010 wet oxidation TOC analyzer). DOC fluorescence was measured in a Turner Designs Model 10 fluorometer, fitted with excitation filters #7-60 and 5G (excitation wavelength 365 nm), emission filter #47-B, and reference filter 2A (emission wavelength 437 nm). Calibration was achieved with quinine sulfate standards and all measurements were converted into quinine sulfate units (qsu), where 1 qsu = 1 μg L^{-1} quinine sulfate in 0.1 M H_2SO_4.

Gross Photoreduction Rate Constants for Freshwaters. If photoreductants are not limiting, then we can assume pseudo-first-order reaction kinetics (eq SI-1 and SI-2) with the associated assumptions outlined. We, therefore, used eq SI-2 to derive the gross photoreduction rate constants.

Derivation of Predictive Model. The derivation of DGM predictive models for UVB and UVA irradiation in both lakes and rivers are outlined in eqs SI-3−SI-9. Using the values calculated in this research and the previous UVB oxidation values of Lalonde et al. (*12*), we propose a general model of mercury photoreduction for lakes and rivers based on the method of O'Driscoll et al. (*5*) for a single reversible reaction.

Validation of DGM Predictive Model for Temperate Lakes. The DGM predictive model for UVB and UVA irradiation of lake water was evaluated using previously published datasets from Puzzle Lake and Big Dam West Lake, Kejimkujik Park, Nova Scotia (*4*) as well as DGM production data from four lakes in Central Quebec (*5*). The Central Quebec dataset (n = 160) was derived using values for UVB and UVA irradiation measured in the field and observed DGM values measured from closed PTFE containers. Therefore, the effects of mixing and volatilization are not a factor. However, in the Kejimkujik data set (n = 119) only total incoming radiation values were available; therefore, we assumed a constant percentage of UVB (0.7%, σ = 0.4) and UVA (13.0%, σ = 3.4) radiation relative to total radiation (based on n = 234 readings in Central Quebec). Also since the Kejimkujik data is continuous DGM measurements sampled from the lake surface we assumed a theoretical 10 × 10 × 10 cm cube in the surface water for calculating incoming radiation energy to a 1 L water sample (or 0.01 m^2 lake surface area). Since mixing effects in the water column, DGM volatilization, and bacterial oxidation of DGM have been shown to be factors affecting DGM concentration in freshwaters primarily close to afternoon (*4*, *10*), we used only the morning DGM data that was collected. Also, since concentrations for reducible mercury were not available, we assumed that 37.8% (SD = 2.7%) of the total dissolved mercury from each lake site was in a reducible form, as derived by the mass balance data in this study.

Log-normalized observed DGM values were compared to log-normalized predicted DGM values using a bivariate scattergram, as outlined by Sokal and Rohlf (eq SI-10, ref *32*).

Results and Discussion

Blanking of System and Mercury Mass Balance. Mercury binding to the sparger was relatively consistent between samples with a mean of 123 pg (SD = 61) mercury bound after each analysis (Table SI-2). Mass balances were performed for North Lake, Ottawa River, St. Lawrence River, and Raison River samples. When the mean value for mercury binding to the sparger was included for samples where there was no data, the mean recovery for all samples was found to be 95% (SD = 33). Since the all mercury was accounted for in the mass balances (within the presented error), we assume we are able to account for all mercury originally present in the samples. Mercury binding to sparger walls is not a source of error in our kinetic calculations since we assume that all mercury converted to DGM at the curve plateau represents all of the mercury that was available for reduction in the sample. In doing so we also assume that

there was no significant binding of DGM to the sparger walls. Of the total mercury available in each sample a mean of 37.8% (SD = 2.7%) was reduced during the experiments (Table SI-2). It is unclear at this time why mercury bound to the sparger walls was unavailable for photoreduction.

Effects of Irradiation Intensity and Breaks in Irradiation. Our kinetic analysis assumes that photoreductants are linked to irradiation but are not reaction limiting. No DGM was produced during short (60 min, Figure 1) and long (24 h) breaks in UVB irradiation. In addition, the DGM production curve showed no additional peak of DGM when irradiation was resumed (i.e. the efficiency of DGM production was not increased after a break in irradiation) (Figure 1). This suggested that the reactants involved in mercury reduction were not being replenished in the dark. Increasing UVB irradiation intensity (61, 90, and 137% average full sun) did not significantly affect the calculated value of k for Ottawa River water implying that photoreductants were not limiting in the DGM production reaction. It should be noted that when elevated concentrations of mercury and solar radiation intensity were used (spiking with 10 000 ng Hg(II) and 583% average UVB radiation), the rate constant was observed to increase slightly (from a mean value of 1.46×10^{-4} s^{-1} (SD $= 3.74 \times 10^{-5}$, $n = 3$) to 2.44×10^{-4} s^{-1}. This result emphasizes the importance of approximating environmental conditions when calculating mercury photoreaction rates.

Further supporting our assumptions regarding photoreductant production, calculated reaction rates of UVA and UVB exposure were not correlated to DOC content ($P > 0.1$, $r^2 < 0.5$). However, exposure to UVA decreased DOC fluorescence from an average of 54 QSU (SE = 25) to 26 (SE = 12) but did not decrease DOC concentrations, 8.34 (SE = 2.69) to 8.24 (SE = 2.67) mg L^{-1}(Table SI-3 and SI-4). If Raisin River is excluded, QSU = 223.9, the UVA mediated decrease is significant ($P < 0.05$), with a decrease from 30 QSU (SE = 6.8) to 15 (SE = 2.8). There were no differences in fluorescence when DOC was exposed to UVB, only decreasing from 51 QSU (SE = 22) to 48 (SE = 20) and the exclusion of Raisin River had no influence on the significance of the effect of UVB irradiation. Similar to UVA, there was no significant decrease in DOC concentrations before and after irradiation with UVB 7.42 (SE = 2.67) to 8.34 (SE = 2.73) mg L^{-1}. The experimental approach used here does not account for structural differences in DOC or associated ions in each system and thus, the lack of relationship between photoreduction rates and DOC concentrations may be confounded by structural differences. In a previous publication (O'Driscoll et al., ref *5*), we used a controlled approach to alter DOC concentrations (but not DOM structure or dissolved ions) within several freshwaters and have demonstrated that DOC is positively related with DGM production efficiency (due to the availability of photoreducible mercury).

Gross Photoreduction Rate Constants for Freshwaters. Given that our assumptions regarding first-order reaction kinetics appear to be valid, the gross photoreduction rate constant k varies between 6.00×10^{-5} s^{-1} and 4.40×10^{-4} s^{-1} for the UVB irradiations, and 5.26×10^{-5} s^{-1} and 3.04×10^{-4} s^{-1} for the UVA irradiations (Table SI-5). A good fit ($r^2 > 0.87$) was observed in all cases between the data and the curve fitting equation and the percentage error was < 4% for each rate constant. The DGM production curves for UVB and UVA radiation are shown in Figure SI-3. The mean rate constant for three Ottawa River UVB replicates was found to be 1.46×10^{-4} s^{-1} (SD = 3.74×10^{-5}). The mean rate constant for all Ottawa River UVA replicates was 6.54×10^{-5} s^{-1} (SD = 1.29×10^{-6}). This suggests an analysis variation of 26% on calculated rate constants for UVB irradiations and 2% for UVA irradiations.

The rate constants appear to divide between lakes and rivers with the mean lake UVB rate constant ($k_{UVB} = 8.91 \times 10^{-5}$ s^{-1}; SE = 3.31×10^{-5}), significantly less (one-way ANOVA $p < 0.085$; Fisher's individual error rate of $P < 0.10$) than the mean rate constant ($k_{UVB} = 1.81 \times 10^{-4}$ s^{-1}; SE = 0.57×10^{-4}) for the river samples. However, while there were differences for the UVB rates between lakes and rivers, the mean and median rate constants for UVA in lakes ($k_{UVA} = 7.76 \times 10^{-5}$ s^{-1}; SE = 1.88×10^{-4}; median $k_{UVA} = 5.94 \times 10^{-5}$ s^{-1}) did not differ significantly (one-way ANOVA $p < 0.361$; Fisher's individual error rate of $P > 0.10$; Kruskas–Wallis test $P < 0.175$) from the mean rate constant ($k_{UVA} = 1.78 \times 10^{-4}$ s^{-1}; SE = 1.03×10^{-4}; median $k_{UVA} = 6.68 \times 10^{-5}$ s^{-1}) for the river sites. The UVA rate constants were nonnormally distributed, but the variances were homogeneous between the river and lake factors. The reason for this difference is not known.

Our work demonstrates that environmentally realistic levels of UVB and UVA radiation result in similar gross mercury photoreduction rates for freshwaters of similar type (either lake or river). The close grouping of the rate constants for both the temperate lakes and rivers analyzed suggests that an accurate general predictive model for gross photoreduction for these freshwaters may be possible. While the data from the arctic lake site (North Lake) was not included in this calculation of the average rate constant for temperate lakes, it is interesting to note that the reaction kinetics were similar to the temperate river systems.

Derivation of DGM Predictive Model. In our models (eqs SI-3–SI-9) we use the value for net photooxidation determined by Lalonde et al. (*12*), who measured a rate constant for UVB photooxidation of 0.25 h^{-1} (or 6.94×10^{-5} s^{-1}) in spiked solutions. Hines and Brezonik (*33*) measured similar rate constants (ranging from 0.39 to 0.76 h^{-1} or from 1.08×10^{-4} to 2.11×10^{-4} s^{-1}) in a small Minnesota lake for mercury photooxidation using an arc lamp radiation source.

It should be noted that while we present data that supports the assumption that photoreduction kinetics are pseudo-first order in nature, we do not currently have data to determine if the same is true for the photooxidation kinetics. Lalonde et al. (*12*, *34*) did observe pseudo-first-order reaction kinetics in a variety of water samples spiked with Hg(0). In addition Lalonde et al. (*34*) found that doubling the intensity of UVB radiation did not alter photooxidation rates. Both observations lend some support to the assumption that photooxidation rates are pseudo-first order in unspiked samples, however this still requires verification.

Since all mercury in the samples was converted to DGM except for that bound to the sparger walls, we will assume that the photoreducible mercury $[Hg_{reducible}]_0$ in a freshwater system is equivalent to 37.8% of the total mercury present in a filtered sample. The mean UVB gross photoreduction rate constant will depend on whether the freshwater is a lake ($k1 = 8.19 \times 10^{-5}$ s^{-1}) or a river ($k1 = 1.81 \times 10^{-4}$ s^{-1}) system (Table SI-5). While there are currently no published values for gross photooxidation rates, we have used the net photooxidation values for UVB determined by Lalonde et al. (*12*) for both river and lake systems ($k2 = 6.94 \times 10^{-5}$ s^{-1}). Therefore, the net DGM production by UVB and UVA radiation in a temperate lakes and rivers can be modeled using the equations provided in the Supporting Information (eqs SI-4–SI-7) and with radiation-based equations SI-8 and SI-9.

As previously discussed the rate constants for photoreduction by UVA were not significantly different for river and lake systems. However we use the individual mean values in these equations in order to be consistent. Using these UVB (eq SI-4 and eq SI-5) and UVA models (eq SI-6 and eq SI-7), DGM dynamics in a river and a lake system containing 1 ng L^{-1} of total reducible mercury were calculated (assumed $[DGM]_0 = 0$ for this exercise) (Figure 2). Upper and lower estimates of DGM concentration were produced using the standard error on the mean gross photoreduction rate

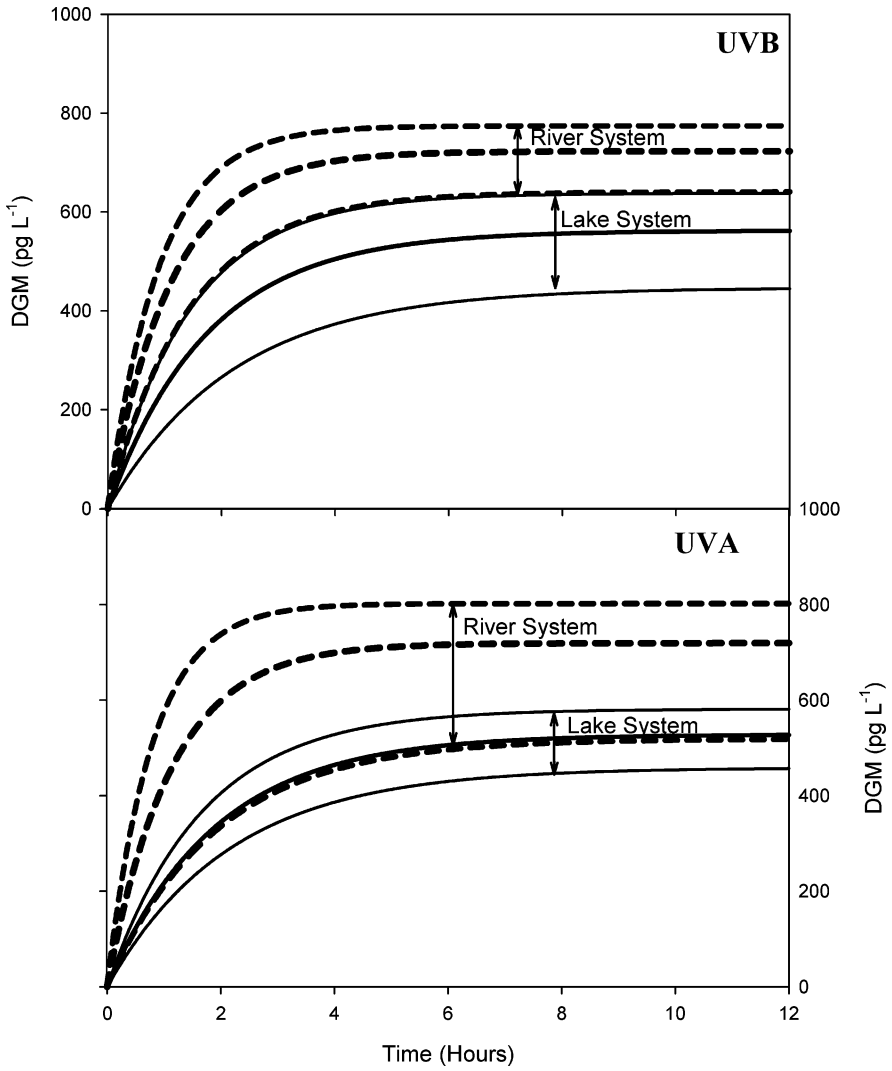

FIGUR E 2. Modeled DGM production in theoretical lake (solid line) and river systems (dashed line) ($[DGM]_0 = 0$ ng L^{-1}, and $[Hg_{reducible}]_0 =$ 1ng L^{-1}) for average UVB (top panel) and UVA (lower panel) radiation used in this study. Range represents standard error on mean rate constants.

constants. Error associated with the photooxidation rate constant is not accounted for. The separation of the model predictions for rivers and lake systems with UVB exposure is illustrated in Figure 2, as is the overlap between model predictions for the river and the lake systems with UVA exposure. The river predictions are still visibly higher for the UVA model.

Validation of DGM Predictive Model for Temperate Lakes. To minimize the effects of volatilization on the data, the lake models were validated using observed DGM data from continuous morning DGM data (8AM−1PM; $n = 119$) collected from Puzzle Lake and Big Dam West Lake (BDW) in Kejimkujik Park, Nova Scotia. In addition, full day data from four lakes in Central Quebec ($n = 160$), where samples were incubated in bottles (so volatilization was not a factor), was used to validate the models (*4*, *5*). For the BDW dataset some splitting of the predicted data was observed, which may be attributed to higher mercury volatilization values recorded on the second day of data collection. The mean daytime (9AM−9PM) mercury volatilization for BDW Lake on day two of field measurements (2.15 ng m^{-2} h^{-1}; SD = 1.72, $n = 36$) was often higher than the mean daytime mercury flux on day one (1.35 ng m^{-2} h^{-1}; SD = 0.69, $n = 36$). Since our model does not account for volatilization this is likely the source of the variation between these 2 days of data.

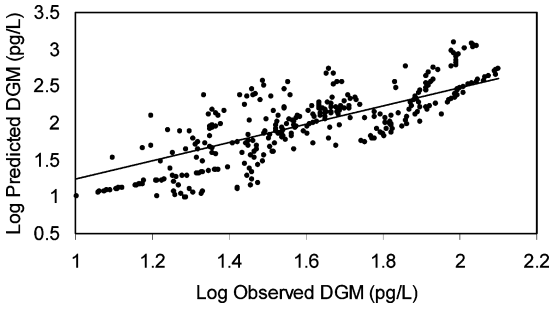

FIGUR E 3. Scatter plot of log-predicted DGM values versus log-observed DGM values from freshwater lakes.

Using principal axis analysis (eq SI-10), a linear fit (correlation = 0.81) was found between log-normalized values for predicted and observed DGM concentrations (Figure 3). A slope of 2.13 (95% confidence interval (CI) range 1.93−2.36) and an intercept of −1.44 (95% CI range −2.07 to −0.81) were obtained for the principal axis. There are several possible explanations for the constant bias observed in the model. It is likely that the major error in applying these DGM models is the estimation of available reducible mercury. The fixed proportion used in our model validation is a likely source of much of the positive bias and suggests that a lower amount of reducible mercury was available in most systems. Mea-

surements of easily reducible mercury (or reactive mercury) in freshwater may be an important measurement for future DGM modeling studies. The use of chemical speciation models for the determination of reducible mercury might also strengthen the predictive abilities of the proposed model and reduce the constant bias observed. This also confirms our previous work that suggests that the role of DOM in controlling reducible mercury is a critical variable in mercury photoredox reactions (*5*).

It should also be noted that these models provide predictions of DGM production in the absence of environmental processes, such as lake mixing and DGM losses due to volatilization. In this study we find that UVB intensity does not alter the rate constant for gross photoreduction. Therefore, the diurnal dynamics observed in field DGM measurements cannot be attributed solely to photoreduction rates. We previously observed that current mercury flux models do not accurately predict DGM volatilization on lakes (*4*). Therefore, we have not incorporated mercury volatilization into the DGM production models presented here. Incorporation of a simple volatilization parameter (e.g., exponential volatilization with respect to DGM concentration) would produce output with diurnal patterns commonly observed in DGM field data. Preliminary data indicates that the diurnal dynamics seen in the O'Driscoll et al. (*4*) dataset can be modeled if we incorporate the loss of DGM due to volatilization using a simple exponential relationship between DGM volatilization and DGM concentration in the surface water. However, as previously noted, more research is required to produce an appropriate flux model that accurately incorporates the effects of volatilization and mixing.

Another source of error in the model predictions may be the use of UVA and UVB irradiation data as opposed to the full spectrum radiation exposure received in a natural setting. Amyot et al. (*7*, *23*) found that UV radiation is the principal component of solar radiation affecting mercury photoreactions in arctic and temperate lakes, however more research is required on the role of visible radiation. Additional error in the model may come from the use of filtered water samples to derive rate constants, as particles and microorganisms (*10*) play a role in mercury reduction in natural systems. Therefore, the rate constants do not reflect interaction with particles and microbiology that may be present in the Kejimkujik field data used to validate the models. Also, as previously noted, since there are currently no published values for gross photooxidation we have used net photooxidation measurements, which likely underestimate the gross oxidation values.

In conclusion this work has developed a laboratory-based controlled system for the determination of the gross photoreduction kinetics of mercury in water. Unspiked freshwater samples were analyzed such that the kinetic analysis results are based on relevant environmental concentrations of mercury. The gross photoreduction rate constants measured for a range of freshwater sites and photooxidation rate constants from the published literature were used to derive predictive models for DGM dynamics in temperate freshwater lake and river systems. The lake model was validated using published data from other temperate freshwater lake sites.

Supporting Information Available

Derivation of gross photoreduction rate constants for freshwaters, derivation of predicted models, statistical analysis of predicted versus measured DGM values, and five tables and three figures showing experimental details. This material is available free of charge via the Internet at http://pubs.acs.org.

Literature Cited

(1) O'Driscoll, N. J.; Rencz, A. N.; Lean, D. R. S. Chapter 14: The biogeochemistry and fate of mercury in natural environments. In: *Metal Ions in Biological Systems*; Sigel, A., Sigel, H., Sigel, R. K. O., Eds.; Marcel Dekker: New York. 2005; Vol 43.

(2) Mason, R. P.; Fitzgerald, W. F.; Morel, F. M. M. The biogeochemical cycling of elemental mercury: Anthropogenic influences. *Geochim. Chosmochim. Acta.* **1994**, *58*, 3191−3198.

(3) Mason, R. P.; Lawson, N. M.; Sheu, G. R. Mercury in the Atlantic Ocean: Actors controlling air-sea exchange of mercury and its distribution in the upper waters. *Deep Sea Res., Part II.* **2001**, *48*, 2829−2853.

(4) O'Driscoll, N. J.; Beauchamp, S.; Siciliano, S. D.; Rencz, A. N.; Lean, D. R. S. Continuous analysis of dissolved gaseous mercury (DGM) and mercury flux in two freshwater lakes in Kejimkujik Park, Nova Scotia: Examining flux models with quantitative data. *Environ. Sci. Technol.* **2003**, *37*(10), 2226−2235.

(5) O'Driscoll, N. J.; Lean, D. R. S.; Loseto, L.; Carignan, R.; Siciliano, S. D. The effect of dissolved organic carbon on the photoproduction of dissolved gaseous mercury in lakes and the potential impacts of forestry. *Environ. Sci. Technol.* **2004**, *38*, 2664−2672.

(6) Amyot, M.; Mierle, G.; Lean, D. R. S.; McQueen, D. J. Sunlight-induced formation of dissolved gaseous mercury in lake waters. *Environ. Sci. Technol.* **1994**, *28*, 2366−2371.

(7) Amyot, M.; Mierle, G.; Lean, D.; McQueen, D. Effect of solar radiation on the formation of dissolved gaseous mercury in temperate lakes. *Geochim. Cosmochim. Acta.* **1997**, *61*(5), 975−987.

(8) Barkay, T.; Turner, R. R.; Van den Brook, A.; Liebert, C. The relationship of Hg(II) volatilization from a freshwater pond to the abundance of mer genes in the gene pool of the indigenous microbial community. *Microb. Ecol.* **1991**, *21*, 151−161.

(9) Vandal, G. M.; Fitzgerald, W. F.; Rolfhus, K. R.; Lambourg, C. H. Modeling the elemental mercury cycle in Pallette Lake, Wisconsin, USA. In: *Mercury as a Global Pollutant: Toward Intergration and Synthesis*; Lewis Publishers: Chelsea, MI, 1994.

(10) Siciliano, S. D.; O'Driscoll, N. J.; Lean, D. R. S. Microbial reduction and oxidation of mercury in freshwater lakes. *Environ. Sci. Technol.* **2002**, *36*, 3064−3068.

(11) Zhang, H.; Lindberg, S. E. Sunlight and iron(III)-induced photochemical production of dissolved gaseous mercury in freshwater. *Environ. Sci. Technol.* **2001**, *35*, 928−935.

(12) Lalonde, J. D.; Amyot, M.; Kraepiel, A. M.; Morel, F. M. M. Photooxidation of Hg(0) in artificial and natural waters. *Environ. Sci. Technol.* **2001**, *35*, 1367−1372.

(13) Krabbenhoft, D. P.; Hurley, J. P.; Olsen, M. L.; Cleckner, L. B. Diel variability of mercury phase and species distributions in the Florida everglades. *Biogeochemistry* **1998**, *40*, 311−325.

(14) Gardfeldt, K.; Feng, X.; Sommar, J.; Lindqvist, O. Total gaseous mercury exchange between air and water at river and sea surfaces in Swedish coastal regions. *Atmos. Env.* **2001**, *35*, 3027−3038.

(15) Gardfeldt, K.; Horvat, M.; Sommar, J.; Kotnik, J.; Fajon, V.; Wangberg, I.; Lindqvist, O. Comparison of procedures for measurements of dissolved gaseous mercury in seawater performed on a Mediterranean cruise. *Anal. Bioanal. Chem.* **2002**, *374*, 1002−1008.

(16) O'Driscoll, N. J.; Siciliano, S.; Lean, D. R. S. Continuous analysis of dissolved gaseous mercury in freshwater ecosystems. *Sci. Total Environ.* **2003**, *304*(1−3), 285−294.

(17) Amyot, M.; Gill, G. A.; Morel, F. M. M. Production and loss of dissolved gaseous mercury in coastal seawater. *Environ. Sci. Technol.* **1997**, *31*, 3606−3611.

(18) Baeyens, W.; Leermakers, M. Elemental mercury concentrations and formation rates in the Scheldt estuary and North Sea. *Mar. Chem.* **1998**, *60*, 257−266.

(19) Costa, M.; Liss, P. S. Photoreduction of mercury in seawater and its possible implications for Hg^0 air-sea fluxes. *Mar. Chem.* **1999**, *68*, 87−95.

(20) Lanzillotta, E.; Ferrara, R. Daily trend of dissolved gaseous mercury concentration in coastal seawater of the Mediterranean Basin. *Chemosphere* **2001**, *45*, 935−940.

(21) Vandal, G. M.; Mason, R. P.; Fitzgerald, W. F. Cycling of volatile mercury in temperate lakes. *Water, Air, Soil Poll.* **1991**, *56*, 791−803.

(22) Amyot, M.; Lean, D. R. S.; Poissant, L.; Doyon, M. Distribution and transformation of elemental mercury in the St. Lawrence River and Lake Ontario. *Can. J. Fish. Aquat. Sci.* **2000**, *57*(Suppl. 1), 155−163.

(23) Amyot, M.; Lean, D.; Mierle, G. Photochemical formation of volatile mercury in high artic lakes. *Environ. Toxicol. Chem.* **1997**, *16*(10), 2054−2063.

(24) Allard, B.; Arsenie, I. Abiotic reduction of mercury by humic substances in aquatic systems—an important process for the mercury cycle. *Water, Air, Soil Poll.* **1991**, *56*, 457−464.

(25) Vette, A. Photochemical influences on the air−water exchange of mercury. Ph.D. Dissertation, University of Michigan, Ann Arbor, MI, 1998.
(26) Rolfhus. The production and distribution of elemental mercury in a coastal marine environment. PhD. Dissertation, University of Connecticut, 1998.
(27) Xiao, Z. D.; Stromberg, D.; Lindqvist, O. Influence of humic substances on photolysis of divalent mercury in aqueous solution. *Water, Air, Soil Poll.* **1995**, *80*, 789−798.
(28) Hintelmann, H.; Evans, R. D. Application of stable isotopes in environmental tracer studies—Measurement of monomethylmercury (CH_3Hg^+) by isotope dilution ICP-MS and detection of species transformation. *Freseniuś J. Anal. Chem.* **1997**, *358*, 378−385.
(29) Siciliano, S. D.; O'Driscoll, N. J.; Lean, D. R. S. Dissolved gaseous mercury profiles in freshwaters. In *Biogeochemistry of environmentally important trace elements*; Cai, Y., Braids, O. C. Eds.; ACS Symposium Series 835; American Chemical Society: Washington, DC, 2002.
(30) Lean, D. R. S.; Siciliano, S. D. Production of methylmercury by solar radiation *J. Phys. IV* **2003**, *107*, 743−747.
(31) Hall, G. E. M.; Pelchat, J. C.; Pelchat, P.; Vaive, J. E. Sample collection, filtration and preservation protocols for the determination of 'total dissolved' mercury in waters. *The Analyst* **2002**, *127*, 674−680.
(32) Sokal, R. R.; Rohlf, F. J. *Biometry: The Principles and Practice of Statistics in Biological Research,* 2nd; W. H. Freeman: San Francisco, CA, 1981.
(33) Hines, N. A.; Brezonik, P. L. Mercury dynamics in a small Northern Minnesota lake: water to air exchange and photoreactions of mercury. *Mar. Chem.* **2004**, *90*, 137−149.
(34) Lalonde, J. D.; Amyot, M.; Orvoine, J.; Morel, F. M. M.; Auclair, J. C-.; Ariya, P. A. Photoinduced oxidation of Hg0(aq) in the waters from the St. Lawrence River estuary. *Environ. Sci. Technol.* **2004**, *32*(2), 508−514.

Received for review June 6, 2005. Revised manuscript received November 7, 2005. Accepted November 22, 2005.

ES051062Y